

Bearing capacity analysis of a shallow foundation with sheet piles under inclined loads by rigid-plastic finite element method

Y. Yamakuri

Department of Civil and Environmental Engineering, Chuo University, Tokyo, Japan

E. Sakon

Graduate School of Natural Science & Technology, Kanazawa University, Kanazawa, Japan (currently Nihonkai Consultant Co., Ltd.)

S. Kobayashi

Institute of Science and Engineering, Kanazawa University, Kanazawa, Japan

H. Nishioka

Department of Civil and Environmental Engineering, Chuo University, Tokyo, Japan

ABSTRACT

A sheet pile foundation (SPF) consists of a footing of a shallow foundation and sheet piles attached to the footing. The vertical bearing capacity of SPF can be increased by the restraining effect of sheet piles on the base ground. SPF exhibits better performance against combined loads, such as seismic loads, in comparison with an ordinary shallow foundation. However, the effect of the restraining effect of sheet piles on the bearing capacity of SPF subjected to these combined loads has not yet been fully understood. In this study, a rigid-plastic finite element method (RPFEM) that is implemented with the bending resistance of the sheet piles was formulated. Subsequently, a series of numerical experiments on the bearing capacity characteristics of SPF subjected to inclined loads was conducted using the proposed RPFEM under various bending strengths of the sheet piles and various joint conditions between the footing and sheet piles. The numerical results revealed that the joint connectivity condition of the footing and sheet piles at the heads has a significant effect on the bearing capacity performance under inclined load.

Key words: *Sheet pile foundation, Ultimate bearing capacity, Inclined loading, Limit analysis, Finite element method*

1. Introduction

A sheet pile foundation (SPF) consists of a footing of a shallow foundation and sheet piles attached to the footing (Nishioka et al., 2010; Nishioka, 2017). From a practical standpoint, SPF is advantageous in terms of construction cost and time because sheet piles, originally temporary retaining works, are an integral part of foundation systems. The vertical bearing capacity of SPF can be increased by the restraining effect of sheet piles on the base ground. Furthermore, SPF shows a better performance against horizontal loads, such as seismic loads, compared with an ordinary shallow foundation because of the bending resistance of the sheet piles.

However, the influence of the restraining effect of sheet piles on the bearing capacity of SPF subjected to inclined or eccentric loadings is not yet fully understood.

The authors developed a numerical code for rigid-plastic finite element method (RPFEM) to solve the bearing capacity and stability problems numerically based on the limit theorem. The formulation of RPFEM is the combination of mathematical optimization and spatial discretization with finite elements. As the rigid-plastic material behavior is assumed, RPFEM requires only the strength parameters and of the soil, cohesion c and internal friction angle ϕ , and the unit-volume weight of the soil self-weight γ , as is similar to Terzaghi's bearing capacity

formula. In contrast to ordinary FEM analysis, RPFEM does not use the elastic parameters, such as Young's modulus E and Poisson's ratio ν in its analysis (Kobayashi, 2005). Therefore, the RPFEM is suitable for evaluating the ultimate limit states, such as the ultimate bearing capacity and failure modes (Pham et al., 2020; Pham et al., 2022; Iqbal et al., 2023). The RPFEM can also be applied to the reinforced ground with tensile-resistant anchors and geotextiles by embedding the restraining effect of the reinforcement members into the ground meshes (Asaoka et al., 1994; Kodaka et al., 1995; Sakon et al., 2021). However, these methods do not consider the finite bending strength of the reinforcement members.

In this study, an RPFEM, including the bending-restraining effects of sheet piles, was developed. Using the proposed RPFEM, a numerical assessment of the bearing capacity characteristics of SPF subjected to inclined loads was conducted to investigate the influences of the joint conditions on the footing and sheet piles and the bending strength of the sheet piles.

2. Formulation of bearing capacity problems of a sheet pile foundation by rigid-plastic FEM

2.1. Rigid-plastic modeling of the reinforcement member

To model reinforcement members such as sheet piles and concrete-facing panels, Kodaka et al. (1995) proposed linear equality constraints with invariant curvature between the three nodes of the ground mesh in contact with the reinforcement members. A conceptual diagram of the curvature-invariant condition is shown in **Fig. 1**. Let the nodal velocities of nodes A, B, and C be $\dot{\mathbf{u}}_A$, $\dot{\mathbf{u}}_B$ and $\dot{\mathbf{u}}_C$ respectively, and the distances between nodes AB and BC be l_{AB} and l_{BC} , respectively. The symbol \mathbf{n} represents the unit vector in the direction of the line segment AC, and the two directions orthogonal to it are s and t . Additionally dt is a small time.

To represent the velocity components in the n , s , and t directions at nodes A, B, and C, respectively, the variables are defined as follows,

$$\begin{aligned} \dot{u}_n^A &= \dot{\mathbf{u}}_A \cdot \mathbf{n}, \dot{u}_s^A = \dot{\mathbf{u}}_A \cdot \mathbf{s}, \dot{u}_t^A = \dot{\mathbf{u}}_A \cdot \mathbf{t} \\ \dot{u}_n^B &= \dot{\mathbf{u}}_B \cdot \mathbf{n}, \dot{u}_s^B = \dot{\mathbf{u}}_B \cdot \mathbf{s}, \dot{u}_t^B = \dot{\mathbf{u}}_B \cdot \mathbf{t} \\ \dot{u}_n^C &= \dot{\mathbf{u}}_C \cdot \mathbf{n}, \dot{u}_s^C = \dot{\mathbf{u}}_C \cdot \mathbf{s}, \dot{u}_t^C = \dot{\mathbf{u}}_C \cdot \mathbf{t} \end{aligned} \quad (1)$$

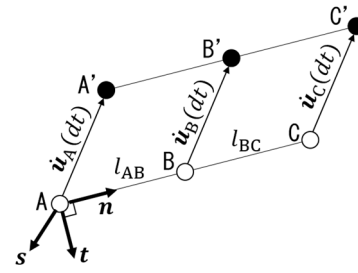


Fig. 1 Conceptual diagram of curvature-invariant condition between three nodes

We focus on the relationship between the nodes A, B, and C on the ns -plane. The gradient (velocity) increment of line AB after deformation is $(\dot{u}_s^B - \dot{u}_s^A) / l_{AB}$, and that of line BC is $(\dot{u}_s^C - \dot{u}_s^B) / l_{BC}$. To be curvature invariant, the gradient (velocity) increments should be equal. Therefore, the following equation is obtained,

$$\frac{\dot{u}_s^B - \dot{u}_s^A}{l_{AB}} - \frac{\dot{u}_s^C - \dot{u}_s^B}{l_{BC}} = 0 \quad (2)$$

Similarly, we obtain the following equation for the t -direction,

$$\frac{\dot{u}_t^B - \dot{u}_t^A}{l_{AB}} - \frac{\dot{u}_t^C - \dot{u}_t^B}{l_{BC}} = 0 \quad (3)$$

When the constraint conditions outlined above are imposed on multiple three-node pairs in a three-dimensional ground mesh, Eqs. (2) and (3) can be transformed to,

$$\mathbf{D}_s \dot{\mathbf{u}}_N = \mathbf{0} \quad (4)$$

where \mathbf{D}_s is an $n_s \times 3n_n$ matrix and, n_s and n_n are the number of constraint conditions and nodes, respectively. Additionally, $\dot{\mathbf{u}}_N$ is a vector that summarizes all nodal displacement velocity fields.

Based on the duality of the problem, the nodal forces owing to the deformation constraints under curvature-invariant conditions, act on the ground mesh.

$$\mathbf{D}_s^T \mathbf{M}_s = \mathbf{f}_s \quad (5)$$

where \mathbf{M}_s is a vector that summarizes all confining forces and corresponds to the bending strength of the sheet piles (Kodaka et al., 1995).

2.2. Rigid-plastic modeling of bending strength of reinforcement member

The following inequality constraints on the confining force were introduced to consider the bending strength of the reinforcement members:

$$-M_m \leq M_{sk} \leq M_m, \forall k \quad (6)$$

where, M_m corresponds to the maximum bending strength value and the lower subscript denotes the k th three-node pair.

2.3. Lagrangian of bearing capacity problems with consideration of reinforcement members

The lower-bound theorem aims to maximize the load factor α while satisfying the equilibrium equation of forces and failure criterion. The Lagrangian for reinforced soil problems, based on the lower-bound theorem of Sakon et al. (2021), is expressed as follows,

$$L = \begin{cases} \alpha + \boldsymbol{\mu} \cdot (\mathbf{B}^T \boldsymbol{\sigma} - \alpha \boldsymbol{\Gamma}_0 - \boldsymbol{\Gamma}_c - \mathbf{D}_d^T \mathbf{p} - \mathbf{D}_r^T \mathbf{q}_r - \mathbf{D}_s^T \mathbf{M}_s) + \boldsymbol{\lambda} \cdot \mathbf{f}(\boldsymbol{\sigma}) + \boldsymbol{\psi} \cdot \mathbf{g}(\mathbf{M}_s) & (\boldsymbol{\lambda}, \boldsymbol{\psi} \geq \mathbf{0}) \\ +\infty & (\text{otherwise}) \end{cases} \quad (7)$$

where variables $\boldsymbol{\mu}$, $\boldsymbol{\lambda}$, and $\boldsymbol{\psi}$ are Lagrangian multipliers. The physical meaning of the right-hand side of Eq. (7) is as follows. The first term is the load factor α . The second term is an equilibrium equation of forces, where \mathbf{B} is a B matrix (used in the general finite element method (FEM)), $\boldsymbol{\sigma}$ represent the stresses at the integration points, $\boldsymbol{\Gamma}_0$ is the reference load, $\boldsymbol{\Gamma}_c$ is a constant load, such as body force,

$\mathbf{D}_d^T \mathbf{p}$ are nodal forces on the Dirichlet boundary

conditions, and $\mathbf{D}_r^T \mathbf{q}_r$ are nodal forces caused by deformation constraints under no-length-change conditions (Asaoka et al., 1994; Kodaka et al., 1995; Sakon et al., 2021). The third term is a failure criterion, where \mathbf{f} is the yield function at the integration points. The fourth term is an inequality constraint condition for the bending strength of the sheet piles, where \mathbf{g} is a convex function corresponding to the bending strength. Note that in the rigid-plastic finite element method based on the upper-bound theorem, no constraint is imposed on M_s because it is difficult to handle inequality constraints. This implies that the bending strength of the sheet piles is sufficiently high. However, in the present formulation, the inequality constraint condition can be handled easily and the bending strength of the sheet piles can be considered.

The following Karush-Kune-Tucker conditions were obtained from the Lagrangian (Eqs. (7)).

$$\text{Equilibrium : } \mathbf{B}^T \boldsymbol{\sigma} = \alpha \boldsymbol{\Gamma}_0 + \boldsymbol{\Gamma}_c + \mathbf{D}_d^T \mathbf{p} + \mathbf{D}_r^T \mathbf{q}_r + \mathbf{D}_s^T \mathbf{M}_s \quad (8a)$$

$$\text{External work rate : } 1 - \boldsymbol{\mu} \cdot \boldsymbol{\Gamma}_0 = 0 \quad (8b)$$

$$\text{Dirichlet boundary : } \mathbf{D}_d \boldsymbol{\mu} = \mathbf{0} \quad (8c)$$

$$\text{Flow rule : } \mathbf{B} \boldsymbol{\mu} = \left(\frac{\partial \mathbf{f}}{\partial \boldsymbol{\sigma}} \right)^T \boldsymbol{\lambda} \quad (8d)$$

$$\text{Complementarity : } \boldsymbol{\lambda} \cdot \mathbf{f}(\boldsymbol{\sigma}) = 0, \boldsymbol{\lambda} \geq \mathbf{0}, \mathbf{f}(\boldsymbol{\sigma}) \leq \mathbf{0} \quad (8e)$$

Moreover, the following terms hold regarding the deformation constraint conditions.

$$\text{Nodal velocity of ground mesh : } \mathbf{D}_r \boldsymbol{\mu} = \mathbf{0} \quad (8f)$$

$$\text{Nodal velocity of ground mesh : } \mathbf{D}_s \boldsymbol{\mu} = - \left(\frac{\partial \mathbf{g}(\mathbf{M}_s)}{\partial \mathbf{M}_s} \right)^T \boldsymbol{\psi} \quad (8g)$$

$$\text{Complementarity : } \boldsymbol{\psi} \cdot \mathbf{g}(\mathbf{M}_s) = 0, \boldsymbol{\psi} \geq \mathbf{0}, \mathbf{g}(\mathbf{M}_s) \leq \mathbf{0} \quad (8h)$$

From the above equations, $\boldsymbol{\mu}$ can be interpreted as the

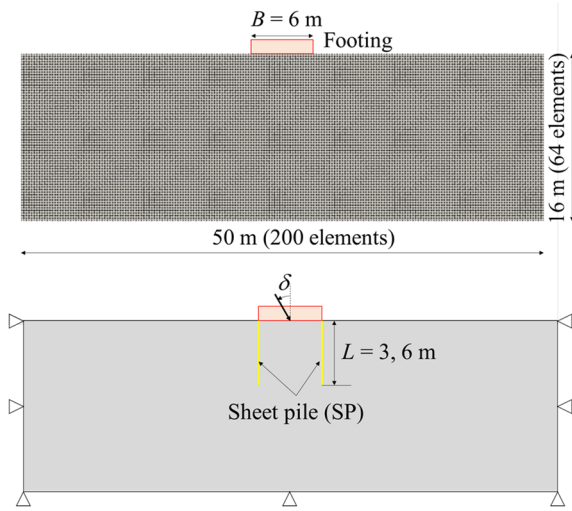


Fig. 2 Finite element mesh and boundary conditions of sheet pile foundation under inclined center load

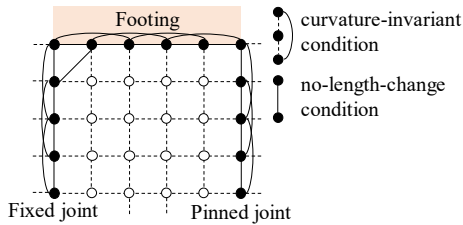


Fig. 3 Rigid plastic model of a sheet pile foundation

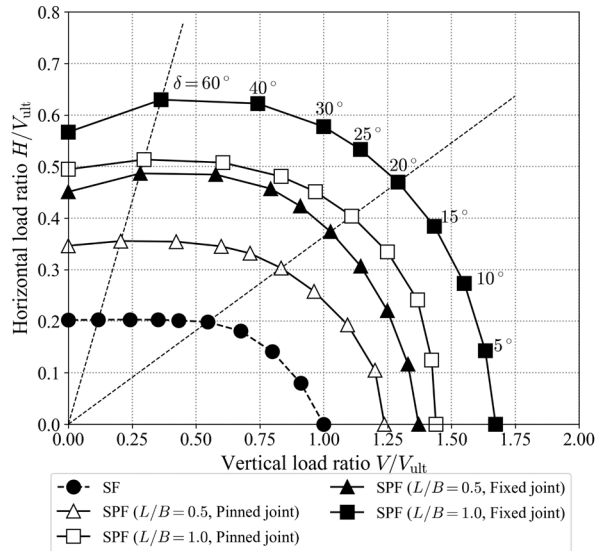
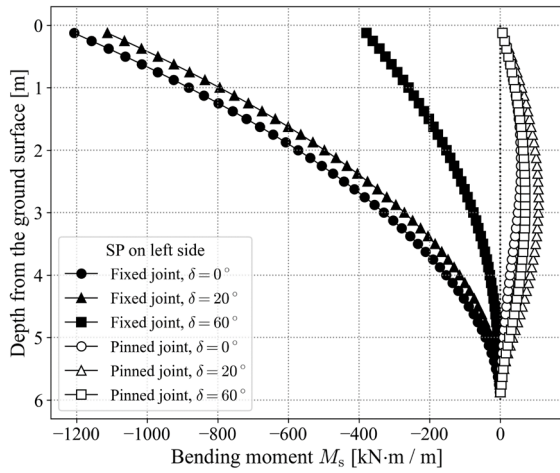


Fig. 4 Influence of joint conditions between footing and sheet piles on failure envelopes in the $H-V$ plane

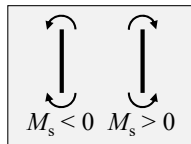
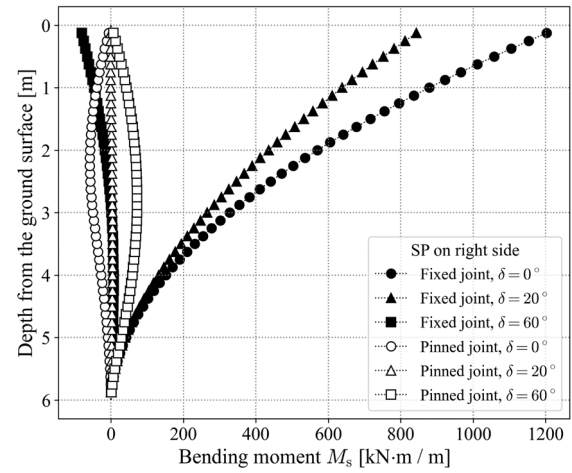


Fig. 5 Distributions of bending strength for pinned joint condition and fixed-joint condition

nodal displacement velocity vector, and λ and ψ as plastic multipliers. In this study, the commercial optimization solver Gurobi Optimizer (Gurobi Optimization, 2023) was used to solve Eq. (7) as the primal problem.

3. Bearing capacity analysis of a sheet pile foundation under an inclined central load

3.1. Influences of joint conditions between footing and sheet piles

First, a series of bearing capacity analyses of sheet

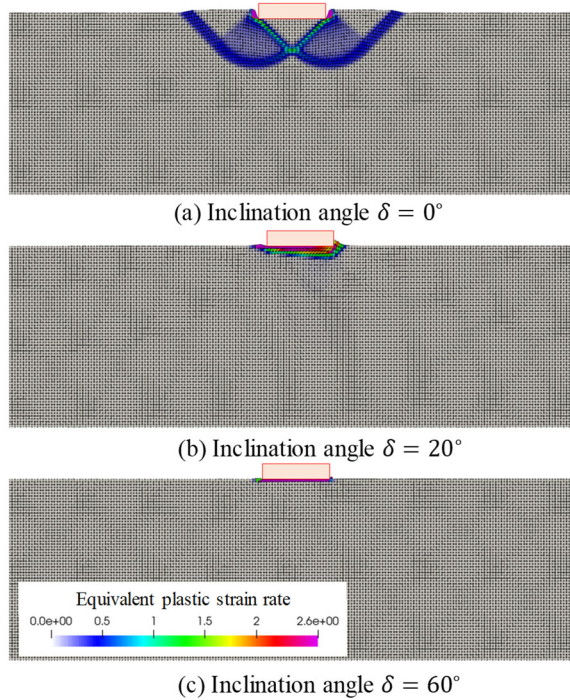


Fig. 6 Deformation diagrams of a shallow foundation without sheet piles

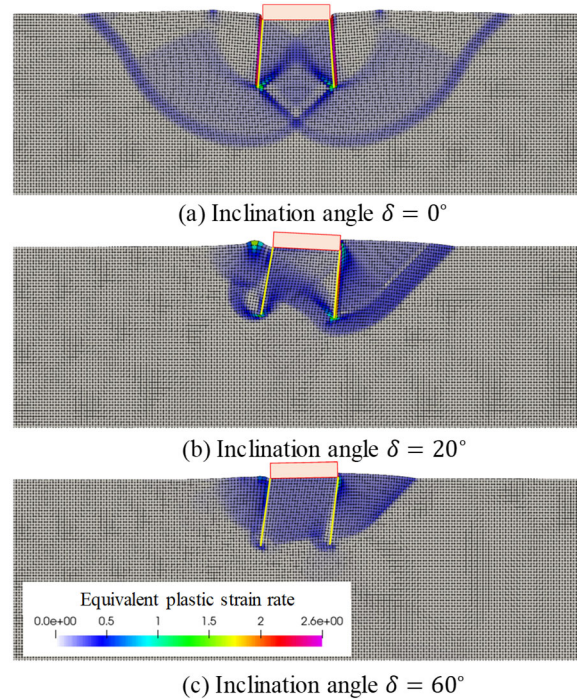


Fig. 7 Deformation diagrams of a sheet pile foundation for the pinned joint condition

pile foundation (SPF) were conducted to investigate the influences of the joint conditions between the footing and sheet piles (SPs). The FE mesh and boundary conditions are shown in **Fig. 2**. It should be noted that numerical analysis in this study was conducted with a three-dimensional code under the plane-strain condition. A 20-node quadratic element was employed for the spatial discretization of the velocity field, and the stress field was evaluated at eight integration points. A total of 12800 elements were used to model the ground. SPF was modeled as shown in **Fig. 3** using curvature-invariant and no-length-change conditions. A rigid rough footing was assumed. A fixed joint condition, which restricted rotation at the pile head, and a pinned joint condition, which allowed rotation at the pile head, were considered. To account for the finite plastic bending strengths of SPs, inequality constraints were imposed on the confining forces in the in-plane direction (i.e., s -direction in **Fig. 1**), which is orthogonal to the member direction (i.e., n -direction in **Fig. 1**). Otherwise, bending strengths are infinite and no plastic bending occurs. Regarding the out-of-plane direction (i.e., t -direction in **Fig. 1**), the plastic bending strength of the SPs were sufficiently large because the analysis should be conducted under the plane-

strain condition. For simplicity, the bending strengths of SPs were assumed to be sufficiently large in this section. The effect of the bending strength of SPs on the bearing capacity characteristics of SPF is discussed in the next section.

A weightless clay ($\phi = 0$), was also considered. Therefore, the von Mises model was used as the failure criterion for the geomaterial, and the inequality constraint $I_1 \leq 0$ was imposed on the first invariant I_1 of the stress tensor to express the tension cut-off (Yamakuri et al., 2020). The cohesion was set to $c = 10 \text{ kN/m}^2$.

The numerical result for various inclination angles δ are summarized as failure envelopes in the H - V plane as shown in **Fig. 4**, where H and V respectively denote the horizontal and vertical components of the ultimate loads. $V_{\text{ult}} (= 52.9 \text{ kN/m})$ is the ultimate bearing capacity of a shallow foundation without sheet piles (SF) for a centered vertical load. This indicates that the size and shape of the failure envelopes in the H - V plane depend on the length of the sheet piles and the joint conditions between the footing and sheet piles. The bearing capacity of SPF under a vertical load ($\delta = 0^\circ$) increased by a maximum of approximately 1.7 times compared with that of the SF. A similar trend was confirmed in the model experiments

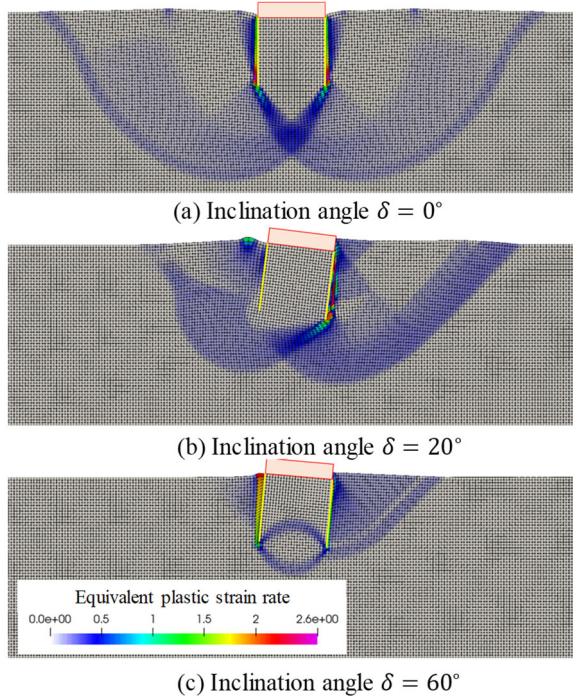


Fig. 8 Deformation diagrams of a sheet pile foundation for the fixed joint condition

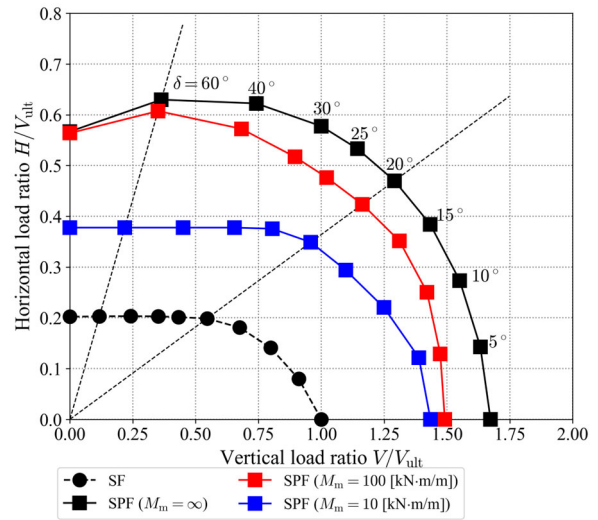


Fig. 9 Influence of bending strength of sheet piles on failure envelopes in the $H-V$ plane for fixed joint condition ($L/B = 1.0$)

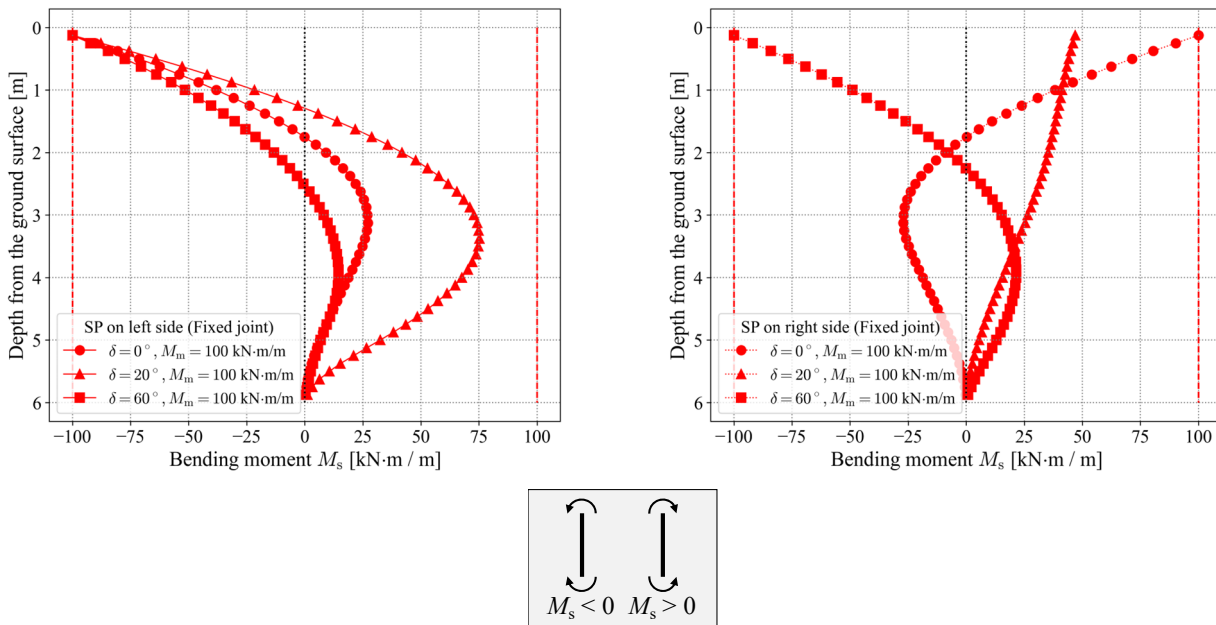


Fig. 10 Distributions of bending strength in the case of fixed joint condition for $M_m = 100 \text{ kN} \cdot \text{m/m}$

conducted using Toyoura sand (Nishioka et al., 2010). Moreover, the bearing capacity of SPF under a horizontal load ($\delta = 90^\circ$) increased by a maximum of approximately three times. It can be observed that the combined use of sheet piles has a greater effect on improving the bearing

capacity for horizontal loads than for vertical loads.

The bending moment distribution obtained by the RPFEM is shown in **Fig. 5**. In the case of the fixed joint condition, the restrained rotation of the pile head exerts bending resistance, which contributes to the improved

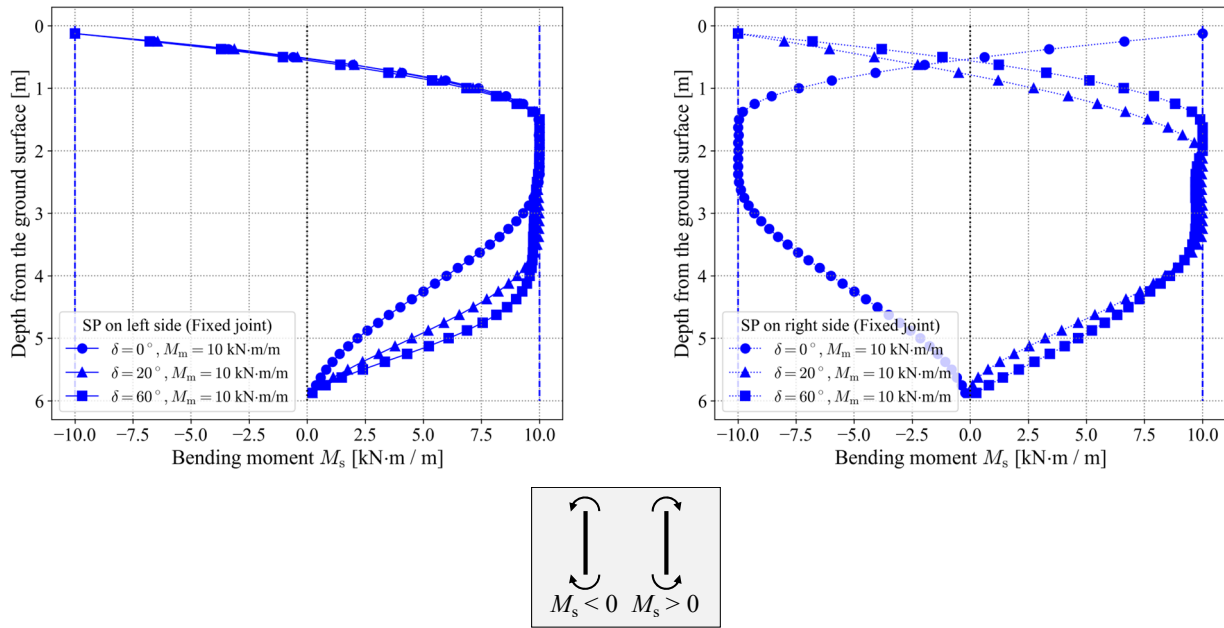


Fig. 11 Distributions of bending strength in the case of fixed joint condition for $M_m = 10 \text{ kN} \cdot \text{m/m}$

bearing capacity. The bending resistance also depends on the load inclination angle. However, in the pinned joint condition, the effect of an improved bearing capacity owing to the bending resistance is less than that in the fixed joint condition because the rotation of the pile head is not restricted.

The deformation diagrams of the SF and SPF are shown in **Figs. 6, 7, and 8**. The results indicated that as the load inclination increases, the failure mode changes from symmetric to asymmetric, and the failure zones become smaller. As shown in **Figs. 7 and 8**, the combined use of sheet piles and footing increases the failure zone. However, the pinned joint condition has a smaller failure zone than the fixed joint condition. This is because the bending resistance of the pile head is low in the pinned joint condition, as mentioned previously. However, in the case of the fixed joint condition, the soil inside the sheet pile exhibits rigid body behavior, which contributes to an improved bearing capacity, as shown in **Fig. 8**.

3.2. Influences of bending strength of sheet piles

We examined the influences of the bending strength of sheet piles under fixed joint conditions ($L/B = 1.0$). The numerical results are presented in **Fig. 9**. The results indicated that the size and shape of the failure envelopes in the H - V plane depend on the bending strength of the sheet piles. However, it can be observed that SPF provides

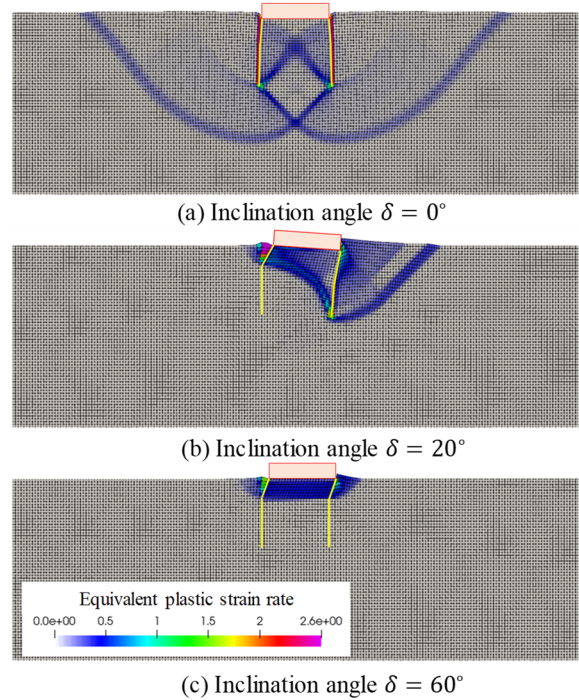


Fig. 12 Deformation diagrams of a sheet pile foundation in the case of fixed joint condition for $M_m = 10 \text{ kN} \cdot \text{m/m}$

a greater ultimate bearing capacity than the SF, although its bending strength is lower.

The bending moment distributions obtained by the RPFEM for $M_m = 100$ and $10 \text{ kN} \cdot \text{m/m}$ are respectively shown in **Figs. 10 and 11**. In the case in which $M_m = 100$

kN · m/m, the moment values reach their limit values at the pile head. In the case in which $M_m = 10$ kN · m/m, the moment values reach the limit values at the pile heads and other points. From these results, it can be understood that as the bending strength decreases, the effect of the improved bearing capacity also decreases.

The deformation diagrams of SPF for $M_m = 10$ kN · m/m, are shown in **Fig. 12**. The failure zone is smaller than that in the case of a sufficiently high bending strength (**Fig. 8**). The bending of the sheet pile occurs because the bending strength reaches its limit, as shown in **Fig. 11**. Moreover, it can be observed that the plastic strain rate is concentrated in the ground inside the sheet pile.

4. Conclusions

This study presented a rigid-plastic finite element formulation that considered the finite bending strength of a reinforcement member, such as sheet piles and concrete-facing panels. It should be noted that this modeling approach requires no specific meshing of the reinforcement members; only the FE mesh of the soil is necessary.

A series of numerical analyses of sheet pile foundation (SPF) subjected to an inclined central load were conducted to investigate the bearing capacity characteristics of SPF subjected to inclined loads. Consequently, the effects of a) the footing and sheet pile joint conditions, and b) the length and bending strength of the sheet piles on the bearing capacity and failure mechanisms were observed. It was confirmed that the combined use of the sheet piles improved the bearing capacity in the horizontal direction more than that in the vertical direction. In particular, the ultimate bearing capacities of SPF were quantitatively evaluated in the form of H - V planes. Based on the findings, it was concluded that the proposed numerical method can be used to evaluate the bearing characteristics of SPF. In future studies, it is desirable to introduce a certain non-dimensional number among strengths and dimensions to express the contribution of bending resistance of sheet piles on the bearing capacities of SPF.

In the future, the proposed method can be used to investigate the bearing capacity characteristics of sheet pile foundations under eccentric loading conditions. Reproduction analyses of the model experiments can be

performed to verify the validity of the proposed method.

References

- Asaoka, A., Kodaka, T. and Pokharel, G., 1994. Stability analysis of reinforced soil structures using Rigid plastic finite element method. *Soils and Foundations*, 34(1), pp. 107-118.
- Gurobi Optimization, LCC, 2023. Gurobi Optimizer Reference Manual, Version 10.0.1. <https://www.gurobi.com/documentation/10.0/refman/index.html> (accessed on 20 December 2023).
- Iqbal, T., Ohtsuka, S., Isobe, K., Fukumoto, Y. and Kaneda, K., 2023. Modified ultimate bearing capacity formula of strip footing on sandy soils considering strength non-linearity depending on stress level. *Soils and Foundations*, 63(3), 101325.
- Kobayashi, S., 2005. Hybrid Type Rigid Plastic Finite Element Analysis for Bearing Capacity Characteristics of Surface Uniform Loading. *Soils and Foundations*, 45(2), pp. 17-27.
- Kodaka, T., Asaoka, A. and Pokharel, G., 1995. Model tests and theoretical analysis of reinforced soil slopes with facing pannels. *Soils and Foundations*, 35(1), pp. 133-145.
- Nishioka, H., Koda, M. Hirao, J. and Higuchi, S. 2010. Vertical and combined loading tests for sheet pile foundation. *International Journal of physical Modeling in Geotechnics*, 10, No. 2, 25-34.
- Nishioka, H., 2017. Development of Sheet Pile Foundation. *IPA News Letter*, 2(4), pp. 13-16.
- Pham, Q. N., Ohtsuka, S., Isobe, K. and Fukumoto, Y., 2020. Limit load space of rigid footing under eccentrically inclined load. *Soils and Foundations*, 60(4), pp. 811-824.
- Pham, Q. N., Ohtsuka, S., Isobe, K. and Fukumoto, Y., 2022. Limit load space of rigid strip footing on cohesive-frictional soil subjected to eccentrically inclined load. *Computers and Geotechnics*, 151, 104956.
- Sakon, E., Yamakuri, Y., Kobayashi, S. and Xiong, X., 2021. Development of Rigid plastic stability analysis for clayey ground reinforced by sheet-like reinforcement. *Journal of Japan Society of Civil Engineers, Ser. A2 (Applied Mechanics (AM))*, 77 (2), pp. I_183-I_192 (in Japanese).

Yamakuri, Y., Kobayashi, S. and Saito, J., 2020. The influence of tensile strength of soils on the bearing capacity analysis by Rigid plastic finite element method. *Journal of Japan Society of Civil Engineers, Ser. A2 (Applied Mechanics (AM))*, 76 (2), pp. I_225-I_236 (in Japanese).